Active control and sound synthesis-two different ways to investigate the influence of the modal parameters of a guitar on its sound

Simon Benacchio, Adrien Mamou-Mani, Baptiste Chomette, Victor Finel

Active control and sound synthesis -

two different ways to investigate the influence

of the modal parameters of a guitar on its sound

Simon Benacchio, Adrien Mamou-Mani, Baptiste Chomette, Victor Finel

Abstract

The vibrational behavior of musical instruments is usually studied using physical modeling and simulations. Recently, active control has proven its efficiency to experimentally modify the dynamical behavior of musical instruments. This approach could also be used as an experimental tool to systematically study fine physical phenomena. This paper proposes to use modal active control as an alternative to sound simulation in order to study the complex case of the coupling between classical guitar strings and soundboard. A comparison between modal active control and sound simulation investigates the advantages, the drawbacks and the limits of these two approaches.

I. INTRODUCTION

Musical instruments are finely tuned mechanical structures involving complex phenomena. The relation between their vibrational properties and sound attributes remains a major question for musical acousticians. Jansson [1] compares the bridge admittance of 25 violins. His aim is to find overall characteristics giving indications of the quality of musical instruments. Results from this kind of measurement campaign are difficult to formalize, as using several instruments involves many uncontrolled physical parameters. Other approaches allow researchers to get around this problem. For instance, Gough [2, 3] compares theoretical predictions based on an analytical model and the measurements of the mechanical admittance of two G-strings mounted on a violin. His aim is to study the coupling between the string and the body of a string instrument. Results about the wolf-note phenomenon and about the two independent modes of transverse vibration of the string are given thanks to the modification of different parameters of both experimental setup and modeling. However, the modal parameters of the soundboard cannot be modified while they have a decisive influence in the coupling between the string and the body. In [4, 5], Woodhouse proposes several sound synthesis methods and validates them comparing with real guitar sounds. One of these methods is then used to find thresholds of perception thanks to modifications of the main parameters of the model [6]. Virtual changes of the modal parameters of the guitar body and of the mechanical parameters of the string give the so-called *just-noticeable differences*. Fritz et al. [7] use the same approach to explore the relationships between acoustical characteristics of violins and their perceived qualities. Wright [8] uses also a sound synthesis method and psychoacoustics tests in order to determine the relative importance of the different acoustical

parameters of the guitar body in the tone quality of the notes played with an instrument. He also says that, thanks to computer synthesis, "the construction parameters can be varied individually in a manner that would be impossible on real instruments". This assertion reveals that active control of vibration was not well-known in the field of musical acoustics in 1996.

Few applications of active control to musical instruments are actually published at this time. Griffin [9] uses active control methods to change the sound of a guitar modifying certain modal properties. He noticeably controls the frequency and the damping of the first three modes of the soundboard, but he does not give their effects on the sound. Later, he also uses active control to cancel the feedback phenomenon when amplified acoustic guitars are played [10]. At the same time, Besnainou [11] modifies the sound of a xylophone bar controlling the phase and the amplitude of its displacement. More recently, Boutin improves this control using a sum of second order band-pass filters in order to modify the amplitudes and the frequencies of the first resonances of a xylophone bar [12]. Using simulations, he also investigates the possible effects of the Proportional-Integral-Derivative control method on a model of a violin "bridge hill" [13]. In [14], Berdahl studies the effect of an active damping applied on the modes of the string of an electric guitar. He succeeds in controlling independently the two transverse modes of the string. These studies reveal that the *in situ* modifications of the mechanical parameters of musical instruments are possible. To the knowledge of the authors no comparison have been made between the active control method, and the well-known sound synthesis method.

This paper deals with the comparison between these two methods in the study of the coupling between a classical guitar strings and soundboard. First, the frequency domain

sound synthesis approach is presented, as well as the modal active control method. The sounding effects of the modal frequency and damping modifications from both methods are compared and discussed. Finally, a short discussion gives the advantages, the drawbacks and the limitations of these two different methods.

II. MOTIVATIONS AND APPROACHES DESCRIPTION

A. The Guitar

The classical guitar chosen for this study is presented in Figure 1. This musical instrument
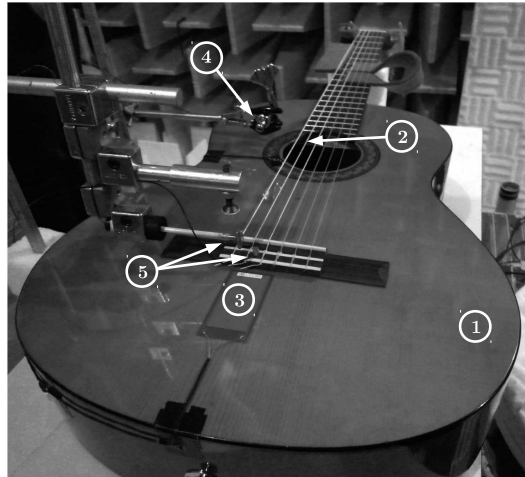

Figure 1: Measurement on the guitar in an anechoic chamber. ① Guitar soundboard, ② A string, ③ Piezoelectric patch used as sensor in the control system (The collocated actuator is fixed inside the body of the guitar), ④ Stand of the thin brass wire used as excitation source, ⑤ Impact hammer and accelerometer used to measure the bridge impedance.

is made up of a lot of parts whose the basic are the strings, the bridge and the body made up of the soundboard, the back, the sides and the air cavity. The small radiating surface of the strings does not allow them to radiate sound directly. The air cavity and the large surface

of the soundboard allow for an efficient radiated sound. The design of the soundboard is then crucial to obtain certain final sound attributes. Selection of soundboard material, shape and assembly with ribs are examples of stages mastered by the guitar maker to target these final sound attributes. This maker know-how implies certain vibrational properties, well characterized in the low frequency region (approximately under 1500 Hz) by its modes of vibration. The fact that the modal parameters of guitars are used for example to discriminate them in different classes [15] motivates the choice of modal approach to compare simulation and active control.

B. Sound Synthesis

The first approach presented in this paper is the sound synthesis method called the frequency domain synthesis. It is based on the model of the string/body coupling in the frequency domain. Then, the inverse Fast Fourier Transform (FFT) is used to find the time-varying transient response of the model. This method proposed by Woodhouse is quickly described here and fully detailed in [4, 5] where all the following equations can be found. This method uses the fact that, when two systems are coupled together at a single point, the admittance $\mathcal{Y}$ of the coupled system defined at this point is given by

$$\frac{1}{\mathcal{Y}} = \frac{1}{\mathcal{Y}_{string}} + \frac{1}{\mathcal{Y}_{body}}, \tag{1}$$

where $\mathcal{Y}_{string}$ and $\mathcal{Y}_{body}$ are the input admittances of the string and the body respectively and defined at the coupling point chosen at the bridge in this case. Using the inverse FFT, this equation gives the time-varying velocity response of the body at the coupling point to an impulse applied to the string. This transfer function is the same as the acceleration

response of the body to a step function force applied to the string. The step function force is a good model of the force applied by a musician on the string when playing. Then a drastic approximation is made to give the sound pressure in the far field of the guitar. According to [16], the sound pressure radiated by a spherical body of radius a moving in the symmetric breathing mode with a uniform velocity V is given by

$$p(r) = V \rho_{air} \, c \, \frac{a}{r} \frac{jka}{1 + jka} e^{-jk(r-a)}, \tag{2}$$

with $k = \omega/c$. c is the speed of the sound and ρ_{air} the density of the air. r is the distance between the center of the spherical body and the point of measurement of the sound pressure. Considering that the acceleration of the sphere is equal to $j\omega V$, the sound pressure is calculated filtering the computed bridge acceleration by

$$R(r) = \frac{1}{j\omega} \left(\rho_{air} \, c \, \frac{a}{r} \frac{jka}{1 + jka} e^{-jk(r-a)} \right). \tag{3}$$

This basic model is used to compute the radiated sound of the synthesized guitar regarding its body as a sphere of radius $a = 20$ cm and with $r = 50$ cm.

The string admittance at the bridge is calculated using

$$\frac{1}{\mathcal{Y}_{string}} = -\frac{iT}{L} \left[\frac{1}{\omega} + \sum_{n=1}^{\infty} \frac{2\omega - i\omega_n \eta_n}{\omega^2 - i\omega\omega_n\eta_n - \omega_n^2} \right], \tag{4}$$

with L and T the string length and tension respectively. ω_n and ν_n are the angular frequency and the loss factor of the nth string mode respectively defined by

$$\omega_n = \frac{i\pi c_s}{L} \left[1 + \frac{B}{2T} \left(\frac{n\pi}{L} \right)^2 \right] \tag{5}$$

and

$$\eta_n = \frac{T(\eta_F + \eta_A/\omega_n) + B\eta_B(n\pi/L)^2}{T + B(n\pi/L)^2}, \tag{6}$$

where $c_s = \sqrt{T/\rho_s}$ is the speed of the wave in the string, B the bending stiffness and η_F, η_A, η_B the coefficients determining friction, air and bending damping respectively. The values of these parameters used for the sound synthesis are extracted from [5] and given in Tables 3 and 4 in Appendix A. However, (4) gives the impedance of the string at the bridge. As the point where the string is plucked is very important for the sound production, the transfer function between the string displacement at the plucking point y_x and the string displacement at the bridge y_L must be added to the model. This transfer function is given by

$$\frac{y_x}{y_L} = \frac{x}{L} + \frac{c}{L} \sum_{n=1}^{\infty} (-1)^n \frac{2\omega sin(n\pi x/L)}{\omega^2 - i\omega\omega_n\eta_n - \omega_n^2}, \tag{7}$$

with x the distance between the guitar head and the plucking point. The admittance of the guitar taking into account this point is given by

$$\mathcal{Y}_{pluck} = \frac{y_x}{y_L}\,\mathcal{Y}. \tag{8}$$

The body admittance $\mathcal{Y}_{body}$ is given by

$$\mathcal{Y}_{body} = \sum_{k=1}^{N} \frac{j\omega}{m_k(\omega_k^2 - \omega^2 + 2j\omega\omega_k\xi_k)} \tag{9}$$

with N the number of modeled modes. ω_k, ξ_k and m_k are the modal frequency, damping factor and effective mass of the kth mode of the body respectively. It is important to note that the effective mass includes the modal mass of the corresponding mode but also the characteristics of the position of the admittance on the guitar. This input admittance is measured at the bridge using an impulse hammer and an accelerometer. Then, modal parameters are identified from this measurement using the Rational Fraction Polynomial (RFP) algorithm [17].

The total transfer function $\mathcal{Y}_{total}$ between the plucking point and the sound pressure is given using the relation (1) between the string admittance (4) and the body admittance (9),

the transfer function between the plucking point and the bridge (7) and the transfer function between the bridge acceleration and the sound pressure (3). The final equation is given by

$$\mathcal{Y}_{total} = \frac{y_x}{y_L} \; \mathcal{Y} \; R(r).$$
(10)

It should be noticed that all parts of the model are time-invariant. Finally, the time-varying transient response of the synthesized guitar is given using the inverse fast Fourier transform (FFT) of the frequency response function given by (10). To sum up, this equation is the transfer function between the string displacement at the plucked position and the radiated sound pressure of the guitar built using the string and the body admittances. As the latters are dependent on frequency, the inverse FFT of (10) is dependent on time and gives the sound of the synthesized guitar. Results of this sound synthesis method are given in section III.

C. Active Control

The second approach presented in this paper is the active control of the guitar soundboard. The technique chosen to control its modal parameters is called the modal active control method [18, 19] and is based on the description of the structure in the modal state space. This method has already proven its efficiency controlling the modal parameters of several musical instruments in different frequency ranges [20, 21]. Its main advantage is to target the energy of the control on the modes of interest using a minimal number of transducers. To ensure the control of all the modal parameters of the soundboard, a proportional and derivative modal state control is used. This technique is quickly described here and fully detailed in [20]. Figure 2 presents the general principle of the modal active control. The vibration of
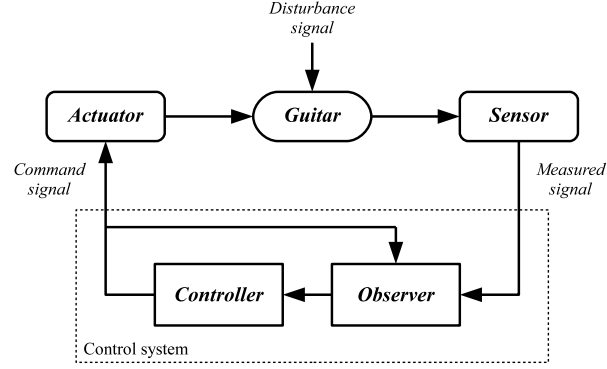
Figure 2: General principle of the modal active control.

the guitar is measured using a sensor bound on the soundboard. This measured signal $y(t)$ is used in the control system to compute the command signal $u(t)$. This signal is added to the disturbance signal $w(t)$ using an actuator and is chosen to modify the parameters of the controlled structure. In this case, the disturbance signal $w(t)$ is created by the string. In the state space, the dynamic of a linear system disturbed and controlled with a proportional and derivative modal state control method can be written

$$
\begin{cases}
\dot{\mathbf{x}}(t) = \mathbf{A}\mathbf{x}(t) + \mathbf{B}u(t) + \mathbf{G}w(t) \\[2mm]
y(t) = \mathbf{C}\mathbf{x}(t) \\[2mm]
u(t) = -\mathbf{K}_1\mathbf{x}(t) - \mathbf{K}_2\dot{\mathbf{x}}(t)
\end{cases}
, \tag{11}
$$

where $\mathbf{x}^t(t) = [\mathbf{q}^t(t)\ \dot{\mathbf{q}}^t(t)]$ is the state vector with $\mathbf{q}(t)$ the vector of the modal displacement. $\mathbf{A}$, $\mathbf{B}$, $\mathbf{C}$ and $\mathbf{G}$ are the matrices of the structure, the input, the output and the disturbance signal respectively. For N modes, one actuator and one sensor, the state matrices can be written

$$\mathbf{A} = \begin{bmatrix} \mathbf{0}_{N,N} & \mathbf{Id}_{N,N} \\ -\mathbf{\Omega}^2 & -2\mathbf{\Xi}\mathbf{\Omega} \end{bmatrix}, \tag{12}$$

$$\mathbf{B} = \begin{bmatrix} \mathbf{0}_{N,1} \\ \mathbf{\Pi}^a \end{bmatrix}, \ \mathbf{G} = \begin{bmatrix} \mathbf{0}_{N,1} \\ \mathbf{\Pi}^w \end{bmatrix}, \ \mathbf{C} = \begin{bmatrix} \mathbf{\Pi}^c \\ \mathbf{0}_{N,1} \end{bmatrix}^t, \tag{13}$$

with $\mathbf{\Omega} = \mathbf{diag}(\omega_k)$ and $\mathbf{\Xi} = \mathbf{diag}(\xi_k)$. The parameters ω_k and ξ_k are the same as in (9). $\mathbf{\Pi}^a$, $\mathbf{\Pi}^c$ and $\mathbf{\Pi}^w$ are the modal vector of the actuator, the sensor and the disturbance respectively. The effective masses presented in (9) are included in the modal vector of the actuator. These parameters are identified from the measured transfer function between the sensor and the actuator using a RFP algorithm.

According to the first equation of (11), the dynamic of the disturbed structure can be modified using the command signal $u(t)$. Thanks to the proportional and derivative modal state control, the modal frequencies, damping factors and effective masses of the structure can be modified. The gain vectors of the controller $\mathbf{K}_1$ and $\mathbf{K}_2$ are chosen using pole placement algorithms adapted for the state [22] and the state-derivative [23] control.

According to the control system described in Figure 2, a Luenberger observer is used [24]. Indeed, the third equation of (11) shows that the command signal is built with the state and the derivative state of the system. As it is not possible to directly measure these two vectors, they are estimated with an observer using the model of the structure. To make sure that the control system is stable, the real part of the poles of the observer are chosen from twice to six times lower than the corresponding poles of the controlled structure. As the observer works with a fixed model of the structure the quality of the estimates and the

accuracy of the control depend on the changes in the nominal system. The model of the structure can be quickly identified before each measurement to improve the efficiency of the control system. Although the observer brings robustness issues, it estimates each modal displacement, velocity and acceleration during control. The control system then targets the energy on modes of interest modifying their modal parameters simultaneously and separately. The dynamic and the design step of the observer are given in [24].

III. COMPARISON BETWEEN SOUND SYNTHESIS AND ACTIVE CONTROL

In order to compare these two approaches the modal frequency and the damping factor of the second mode of the soundboard of the guitar are modified. The frequency of this mode is 213 Hz. The effects of the control in the sound are studied investigating the coupling between this mode and the second partial of the A string of the guitar since its frequency is 220 Hz and roughly matches the frequency of the controlled mode. This mode is chosen for its important role in the sound of the instrument. Its large amplitude is significant for the mastering of the amplitude and the decay of several fundamental and second partials of the guitar. The study focuses on this frequency range and on the coupling phenomenon to achieve an accurate and detailed comparison of the control and synthesis approaches. The proposed illustration is a specific case of coupling. Other modifications of the modal parameters of the soundboard should be performed in other frequency ranges to generalize the results regarding the coupling phenomenon between a string and the modes of a soundboard. In this paper, several modifications of the damping factor and of the frequency are studied and compared when applied using the synthesis method or the active control.

- In the case of sound synthesis, the modal parameters are directly modified in the impedance of the soundboard changing the parameters of (9). The initial values of these modal parameters are the same that those of the control system described in the next paragraph. Then the synthesized radiated sound of the guitar is calculated using the method presented in section II.

- In the case of active control, the control system is designed to match the targeted modifications using a pole placement algorithm. To modify the sound of the guitar, the real part of the poles can be placed close to zero (for example to decrease the damping factor of a mode). Thus, the stability margins of the control system are sometimes decreased but always kept large enough to maintain its stability. The modal model of the soundboard is built using 23 modes identified using the measured impedance. The large number of modes used in the model avoids strong spillover effects in the studied range of frequency. The identified parameters of the first ten modes and the corresponding values of B and C are given in Table 5 in Appendix A. The bridge impedance is measured using an integrated signal from an accelerometer and an impact hammer. The radiated sound is measured 50 cm in front of the soundboard using a microphone. The string excitation is produced using thin brass wire which is attached to the string 15 cm from the bridge. Pulling this wire until it breaks gives a repeatable plucked string excitation. The experimental setup is presented in Figure 1.

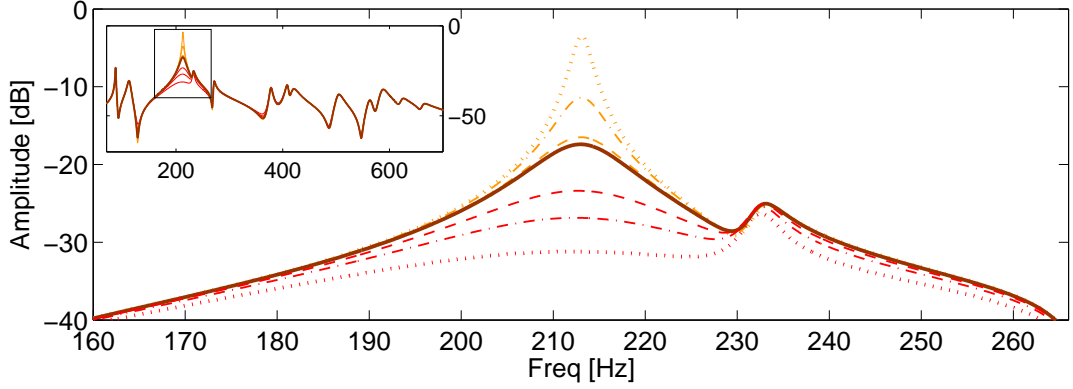## A. Modification of the Damping Factor

The first comparison between the two proposed approaches is done on the damping factor

| Targeted shift [%]	-80	-50	-10	0	+100	+200	+400
Damping factor [] Synthesis	0.005	0.013	0.023	0.025	0.05	0.075	0.126
Control	0.013	0.017	0.024	0.025	0.047	0.057	0.072

Table 1: Values of the damping factor of the soundboard mode for the synthesis and the control methods.

of the second mode of the soundboard. Seven cases are studied. The damping factor of the targeted mode is altered by $+400\%$, $+200\%$, $+100\%$, 0%, -10%, -50% and -80%. The case with no modification is called the reference case. Figure 3 gives the synthesized and the measured bridge impedance of the guitar for these different cases. These two figures focus only on the targeted mode to make them more readable. Inserts show the studied frequency range in larger views of the transfer functions. These figures show that the two approaches are efficient. The active control method seems to be slightly less accurate than the synthesis method. Indeed, Figure 3(b) shows that the control of the damping factor slightly modifies the frequency of the controlled mode. This might be due to an approximate identification of this mode for the model used to design the control system. The values of the damping factor after the modifications are given in Table 1 for the control and the synthesis methods.

To further investigate the control efficiency, Figure 4 gives the upper part of the targeted and actual pole locations of the controlled mode. The non-circled symbols give the targeted locations and match the nearly horizontal dotted line which is the locus of equal frequency locations. The circled symbols give the actual pole locations of the controlled mode. As they don't match the nearly horizontal line, the frequency of the controlled mode is also modified.

(a) Synthesized bridge impedances - Synthesis approach.
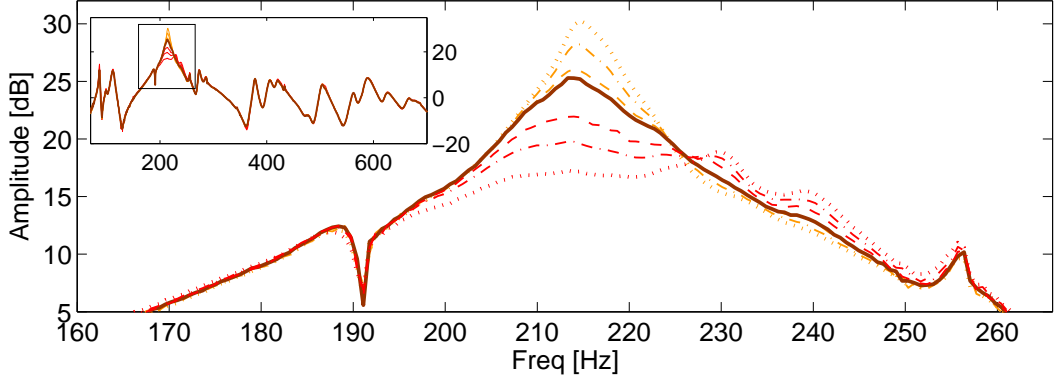
(b) Measured bridge impedances - Active control approach.

Figure 3: Modifications of the damping factor of the second mode in the soundboard impedance. Reference case [——], damping factor altered by +400% [·····], +200% [·—], +100% [— —] and damping factor altered by −10% [— —], −50% [·—], −80% [·····].

The system is stable since the real parts of the poles are always under zero. If one looks at the other poles of the system this stability criterion is also observed. However, if the damping factor of the mode decreases more than −80%, the real part of the pole could be too close to zero and the system could be unstable.

Then, the sounds produced using the two methods are studied. The spectrum of the
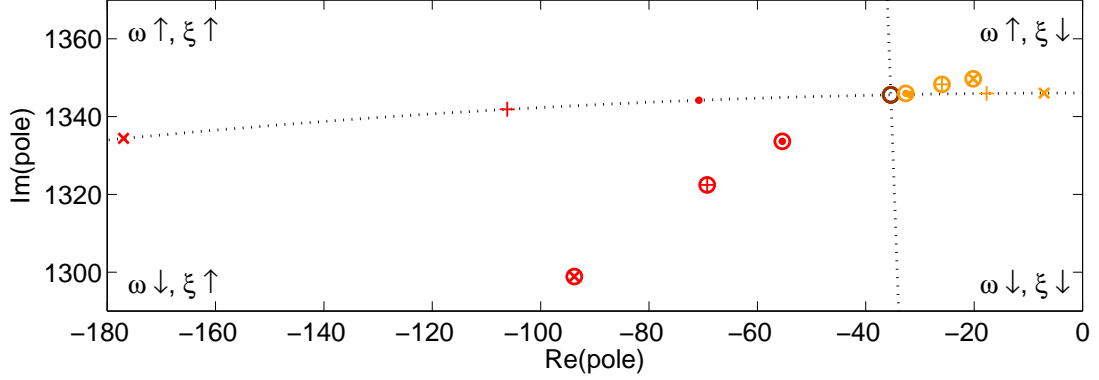
Figure 4: Pole locations of the controlled mode. Reference case ○, damping factor altered by +400% [·,⊙], +200% [+,⊕], +100% [×,⊗] and damping factor altered by −10% [·,⊙], −50% [+,⊕], −80% [×,⊗]. The non-circled and circled symbols indicate the poles at the targeted and the actual location of the controlled mode respectively. The nearly horizontal and nearly vertical dotted lines give the locations where the frequency and the damping factor of the controlled mode are kept unchanged respectively.

synthesized sound and the Fourier Transform of the measured radiated sound are presented in Figure 5. Again, these two figures focus on the second partial of the played note. Once again the two approaches give similar results. The coupling between the string and the guitar body is clearly modified when the damping factor of the body mode is shifted. The body/string coupling phenomenon is fully described by Gough in [2]. When decreasing, the damping factor increases the coupling between the body and the string modes. According to Gough, these two modes can be either strongly or weakly coupled. For a strong coupling, the decrease of the damping factor of one of these modes creates two peaks. Their frequencies move away and their damping factors decrease together. This is clearly the case of the −50% and −80% shifts of the damping factor. The reference case and the −10% shift are also cases
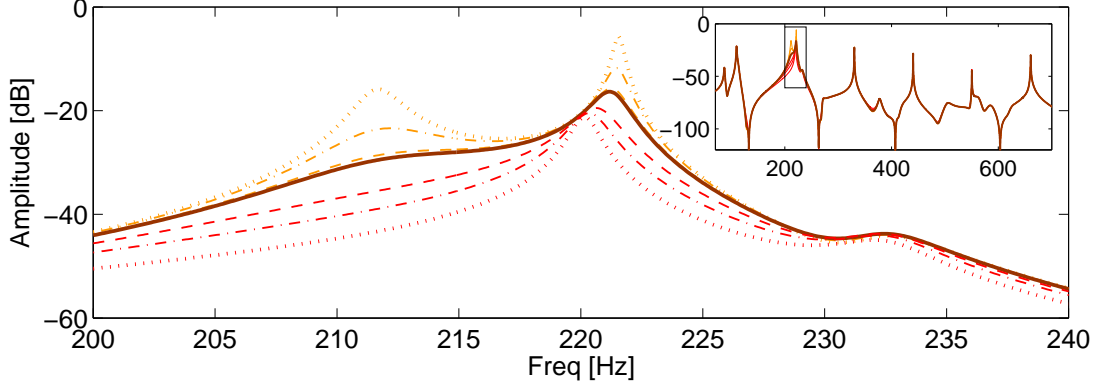
(a) Spectrum of the synthesized radiated sound.
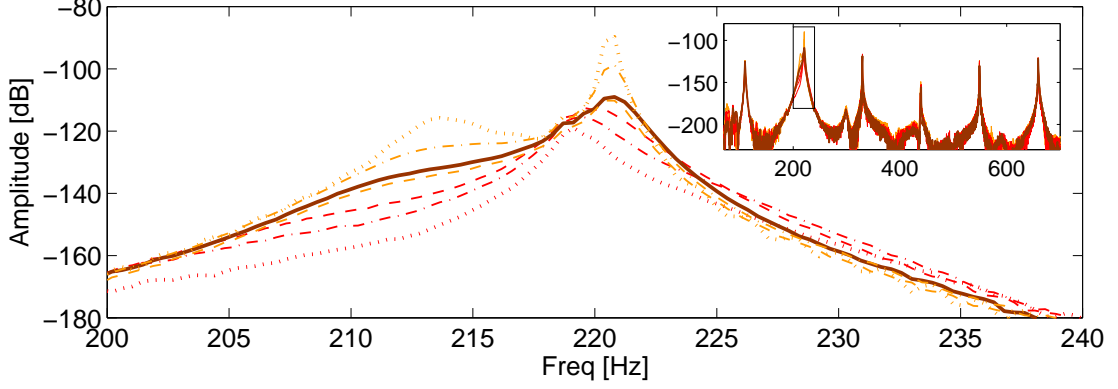
(b) Fourier Transform of the measured radiated sound of the controlled guitar.

Figure 5: Comparison between the radiated sound for the synthesis and the active control. Reference case [——], damping factor altered by $+400\%$ [······], $+200\%$ [·—·], $+100\%$ [— —] and damping factor altered by -10% [— —], -50% [·—·], -80% [······].

of strong coupling since the damping factor of the visible peaks in Figure 5 decreases when the damping factor of the body mode decreases. The $+100\%$, $+200\%$ and $+400\%$ shifts are cases of weak coupling. Indeed, according to Gough [2], when the damping factor of the body mode lower in frequency than the string partial decreases, the frequency and the damping factor of the partial increase. This is clearly the case of these three last shifts of the damping

factor as shown in Figure 5.

To support these observations, the temporal envelope for the second partial of the string is given in Figure 6 for the seven modifications of the damping factor. These temporal envelopes are extracted from the spectrograms of the synthesized and measured sounds. They represent the time evolution of the energy of the targeted partial. This figure shows a
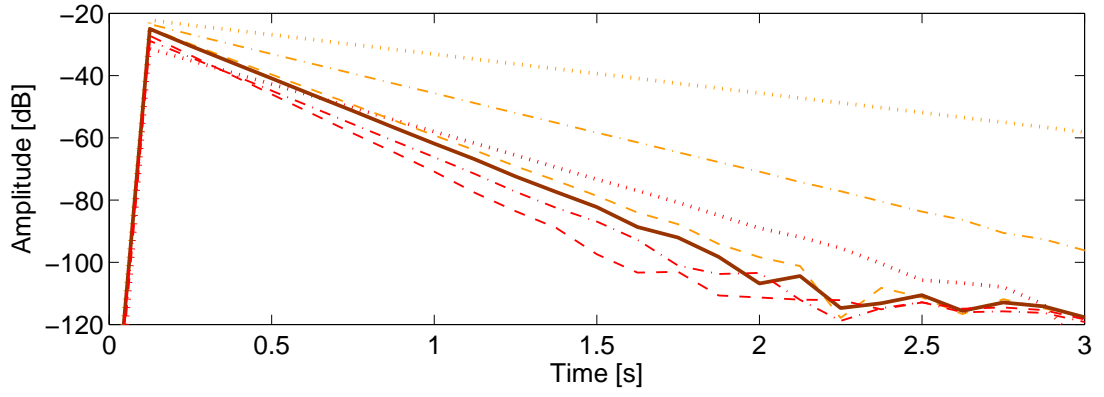
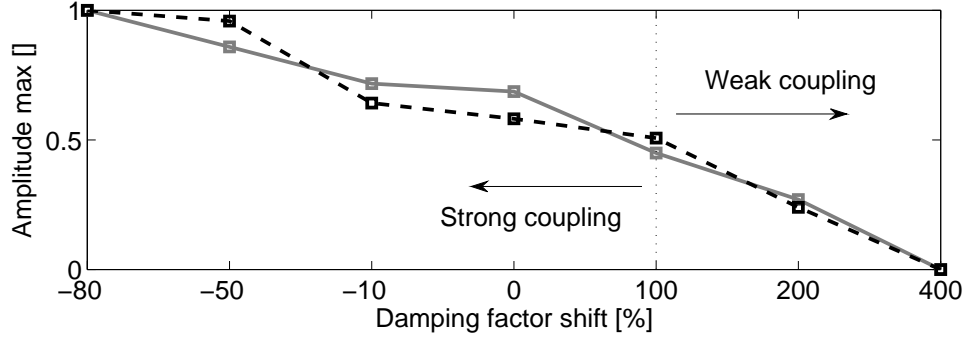

(a) Synthesized temporal envelope - Synthesis approach.
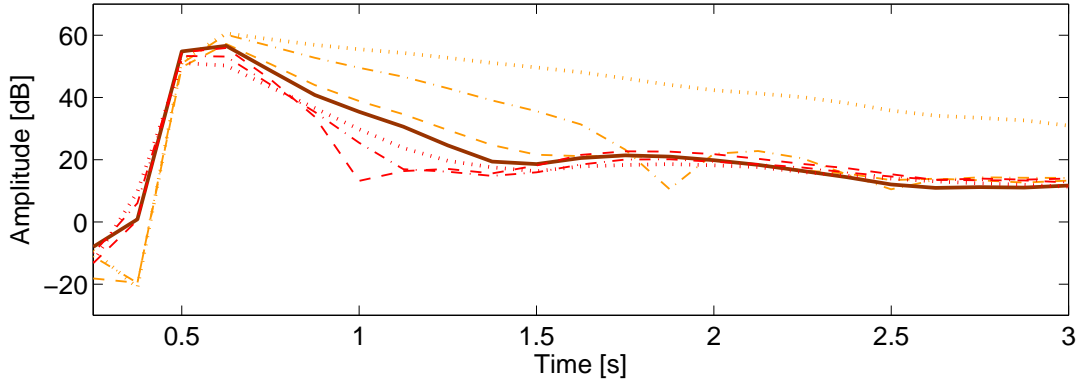
(b) Measured temporal envelope - Active control approach.

Figure 6: Temporal envelope of the second partial of the A string. Reference case [——], damping factor altered by +400% [....], +200% [._.], +100% [_ _] and damping factor altered by −10% [_ _], −50% [._], −80% [....].

good similarity between the two approaches. Moreover, it can be seen that the $+100\%$ shift is the limit between the strong and the weak coupling since the slope of the corresponding time evolution is the largest. Once again, Figure 6(b) shows that the control approach is more variable than the synthesis approach. The temporal envelope of the measured sound is much more complex than the time evolution of the synthesized sound. For example, the curves in Figure 6(a) are straight while some curves in Figure 6(b) present bounces. This might be due to the polarization of the string, which is not included in the model used in sound synthesis. This phenomenon is described in [4].

The comparison between the controlled and synthesized temporal envelopes given in Figure 6 is difficult. The main characteristics of these curves are detailed in Figure 7 in order to better observe the coupling modification as a function of the modal parameter shifts. Figure 7 gives the maximum amplitude and the slope of the temporal envelope of the second partial of the string in the different studied cases. The maximum amplitudes are normalized between 0 and 1 since the scales of the spectrum of the synthesized sound and the Fourier Transform of the measured sound are not the same. The slopes are calculated using 0.5 second of the temporal envelope after their maximum amplitudes. Only the transient of the partials is studied since it is known to be very important regarding the sound attributes of musical instruments. Arrows indicate the observed coupling behavior also predicted by Gough's model. Once again the results are similar. Figure 7(a) reveals that the stronger is the coupling between the body and the string modes the higher is the amplitude of the coupled partial. Figure 7(b) supports the fact that the $+100\%$ shift is the limit between the strong and the weak coupling since the slope is the largest for this case. This observation reveals also that the coupling in the reference case is strong since all the points to the left

(a) Maximum amplitude normalized between 0 and 1.
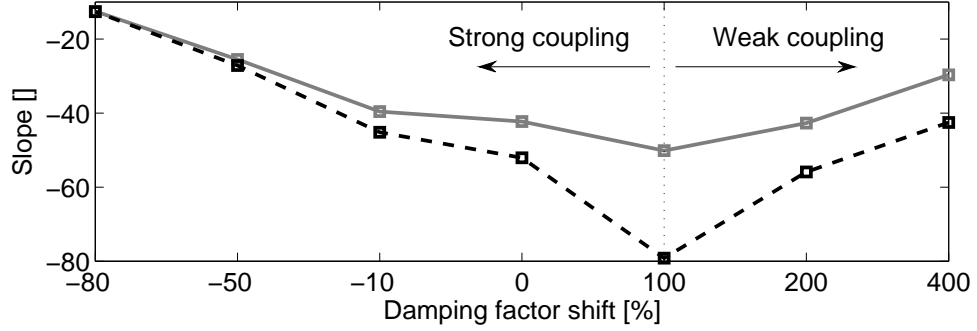
(b) Slope calculated using 0.5 second of the temporal envelope after its maximum amplitude.

Figure 7: Maximum amplitude and slope of the temporal envelopes given in Figure 6 for the synthesis approach [——] and the control approach [- - -] and for the different shifts of the damping factor.

of the point corresponding to the +100% shift are strongly coupled. It should be noticed that the results of the modification of the coupling between the string and the mode of the soundboard depends on the initial value of the damping factor. Indeed, the control of another mode in another frequency range could lead to other observations since the initial coupling would be different.

B. Modification of the Modal Frequency

The second illustration of the two proposed approaches is done for the modal frequency of the second mode of the soundboard. The principle is the same as in the previous section. In addition to the reference case, the frequency of the mode is altered by $\pm 5\%$, $\pm 10\%$ and $\pm 15\%$. Figure 8(a) gives the seven impedances used in the synthesis model and Figure 8(b) gives the controlled impedances measured at the bridge. For clarity, these two figures focus only on the targeted mode. Inserts show the studied frequency range in larger views of the transfer functions. These figures show that the synthesis and the active control give close results. The values of the frequency after the modifications and the actual shifts in Hertz are given in Table 2 for the control and the synthesis methods. It should be noticed that the frequency shifts in Hertz depends on the location of the controlled mode across the range of frequencies. To control the frequency of another mode the shifts in percent should be adapted to the frequency range of work. The synthesis approach gives expected results while those of the control approach are less precise. The targets in percent are not perfectly reached for the active control method. This might be due to computation errors during the design of the control system, the use of a non perfect model or the influence of the residual modes. The curves matching the $+10\%$ and $+15\%$ shifts show that the small mode located at a frequency of 240 Hz has not a negligible influence on the results. Indeed, its amplitude increases when the modified mode is shifted to higher frequencies. In active control applications this usual phenomenon is known as the spillover effect. It is due to the imprecise modeling of the modes which are not much excited during the identification step. Then, a part of the energy used to modify the controlled mode is passed to these modes unintentionally increasing their amplitudes. However, even if the shift to high frequencies is disturbed by the mode located at 240 Hz, the amplitude increase makes the controlled impedance not so far from
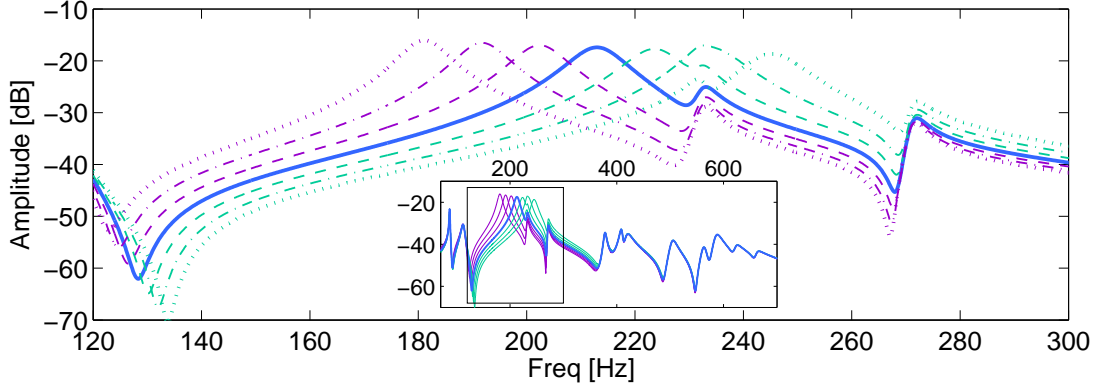
(a) Synthesized bridge impedances - Synthesis approach.
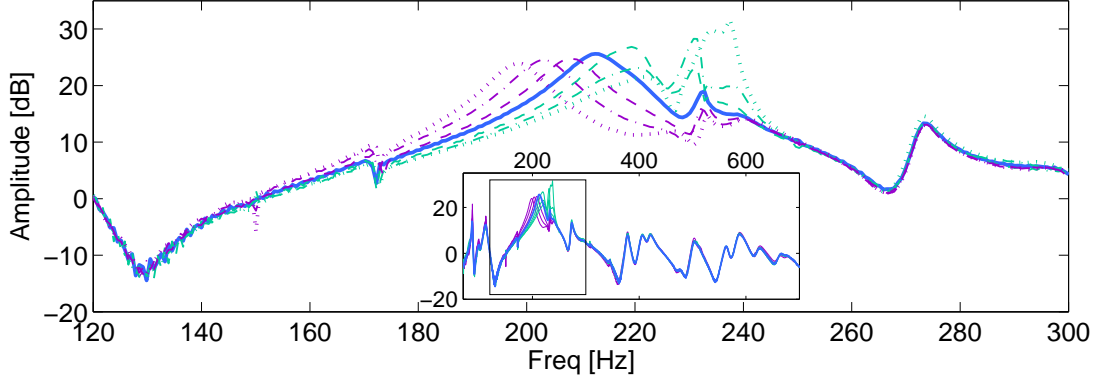
(b) Measured bridge impedances - Active control approach.

Figure 8: Modifications of the frequency of the second mode in the soundboard impedance. Reference case [——], frequency altered by -15% [·····], -10% [·—], -5% [— —] and frequency altered by $+5\%$ [— —], $+10\%$ [·—], $+15\%$ [·····].

the synthesized one. The digital damping is also a usual constraint of active control systems. As this changes the damping factor of the controlled mode, the control system is designed to keep the modal damping factor constant.

The upper part of the targeted (non-circled symbols) and actual (circled symbols) pole locations of the controlled mode are given in Figure 9. The nearly vertical line gives the

Targeted shift [%]		-15	-10	-5	0	+5	+10	+15
Frequency [Hz]	Synthesis	181	192	202	213	224	234	245
	Control	199	203	209	213	219	221	222
Shift [Hz]	Synthesis	-32	-21	-11	0	+11	+21	+32
	Control	-14	-10	-4	0	+6	+8	+9

Table 2: Values of the frequency of the soundboard mode around 213 Hz for the synthesis and the control methods.

locus of equal damping factor locations. The poles of the shifts to low frequencies and to high frequencies respectively stay close to and move away from this line. The damping factor is clearly modified for the cases where the frequency is increased. Figure 9 also gives the unexpected pole modifications of the small mode located at 240 Hz. The damping factor of this mode decreases when the damping factor of the controlled mode increases and vice versa. This might be due to the spillover effect. However, this effect is accentuated by the coupling between the two modes. Indeed, the modification of the damping factor of the small mode when the controlled mode is shifted in low frequencies reveals a coupling between these two modes. The spillover effect also limits the frequency shift of the controlled mode since the real part of the pole of the small mode could be shifted too close to zero and could make the system unstable.

Then, the sounds produced using the two proposed approaches are studied. Figure 10(a) gives the spectrum of the synthesized sounds. Figure 10(b) gives the Fourier Transform of the radiated sounds measured in front of the guitar. To be clearer, these two figures focus on the
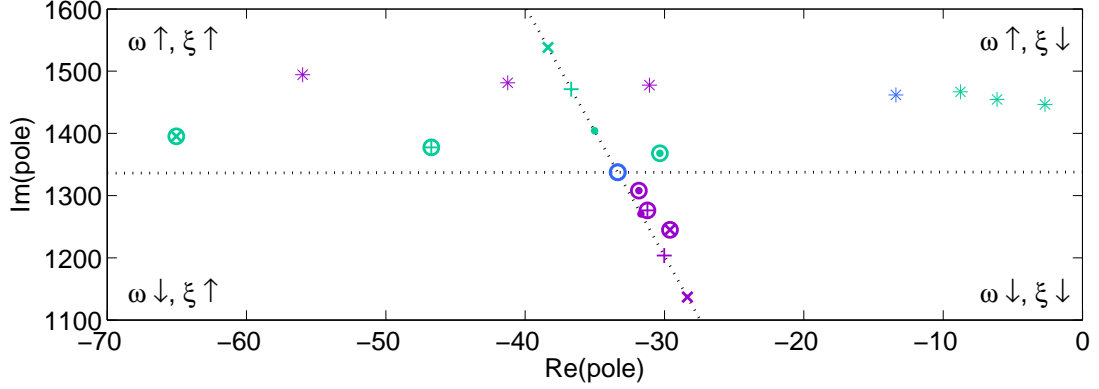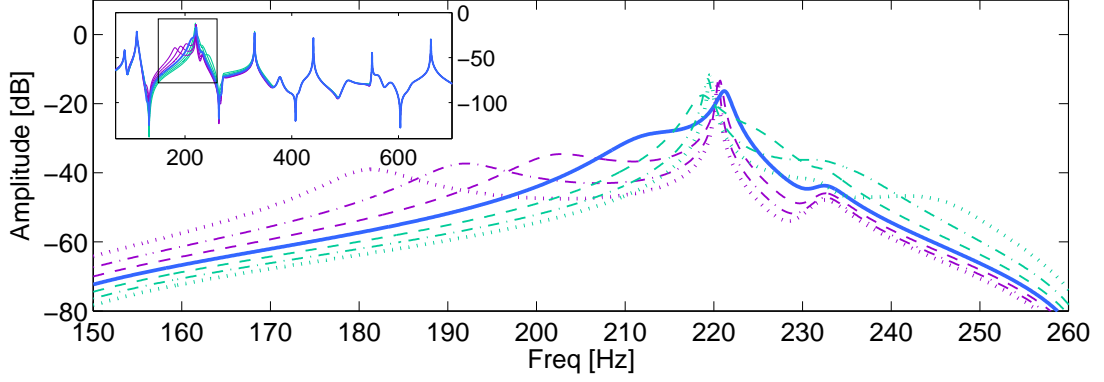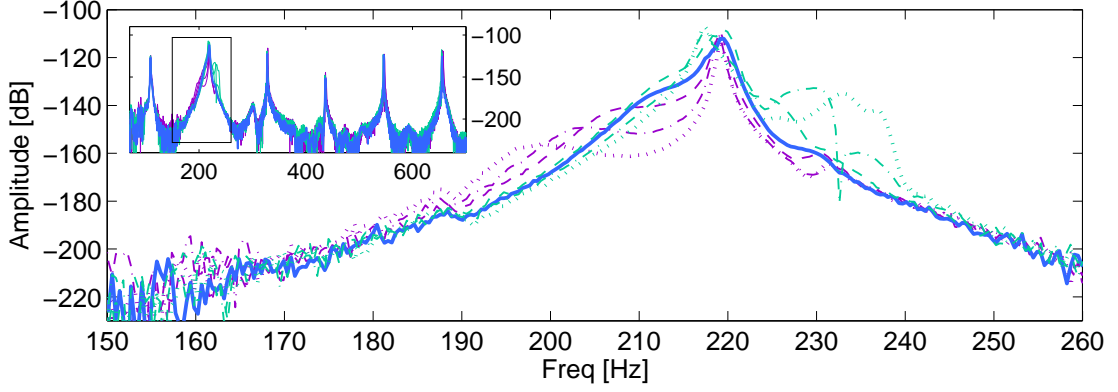
Figure 9: Pole locations of the controlled mode. Reference case ○, frequency altered by −15% [×,⊗], −10% [+,⊕], −5% [·,⊙] and frequency altered by +5% [·,⊙], +10% [+,⊕], +15% [×,⊗]. The non-circled and circled symbols indicate the poles at the targeted and the actual location of the controlled mode respectively. The nearly horizontal and nearly vertical dotted lines give the locations where the frequency and the damping factor of the controlled mode are kept unchanged respectively. The [∗] give the unexpected modifications of the pole of the mode located at 240 Hz during control.

second partial of the played note. The effects of the frequency shift on the partial of the string are similar for the synthesized and the measured sounds. The results observed in Figure 10 indicate that the body and the string modes are strongly coupled. As described by Gough [2], when the frequency of the body mode is shifted far away from the frequency of the string partial, the latter is slightly shifted from its original frequency. When the string partial is lower than the body mode, its frequency slightly decreases. When the string partial is higher than the body mode, its frequency slightly increases. When the frequency of the body mode roughly matches the frequency of the string partial, the coupling becomes stronger. In this case, it is more difficult to discriminate between the two modes. This is the case in Figure

(a) Spectrum of the synthesized radiated sound.

(b) Fourier Transform of the measured radiated sound of the controlled guitar.

Figure 10: Comparison between the radiated sound for the synthesis and the active control. Reference case [——], frequency altered by −15% [……], −10% [·—], −5% [— —] and frequency altered by +5% [— —], +10% [·—], +15% [……].

10 for the reference sound and for the +5% shift of the frequency.

Then, the effects of these modifications in the temporal envelope of the second partial of the A string are studied. Figure 11 presents the first three seconds of the synthesized and measured temporal envelopes in the seven cases presented in Figure 8. Again, the behavior of the temporal envelopes are close. As in Figure 8, the effects of the frequency shift are
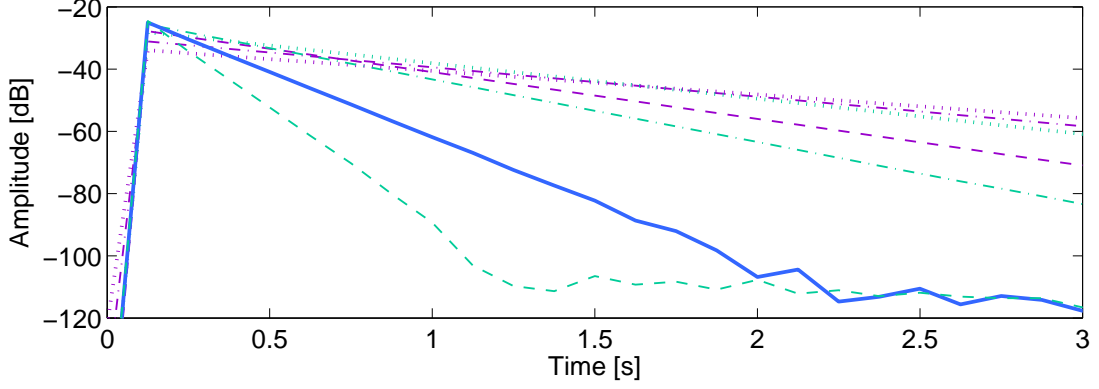
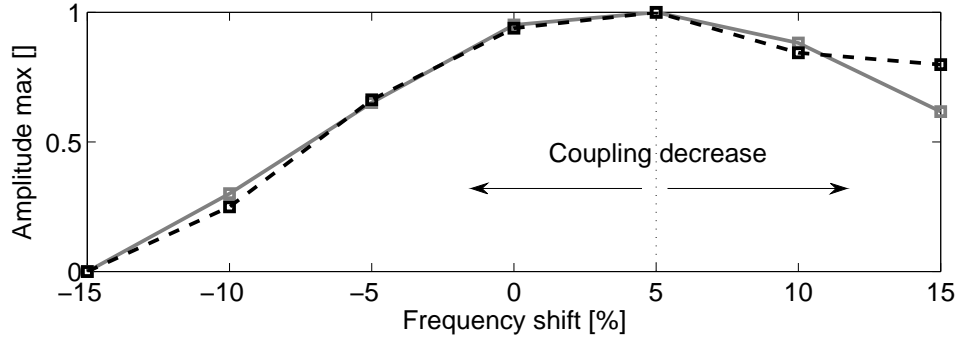(a) Synthesized temporal envelopes - Synthesis approach.
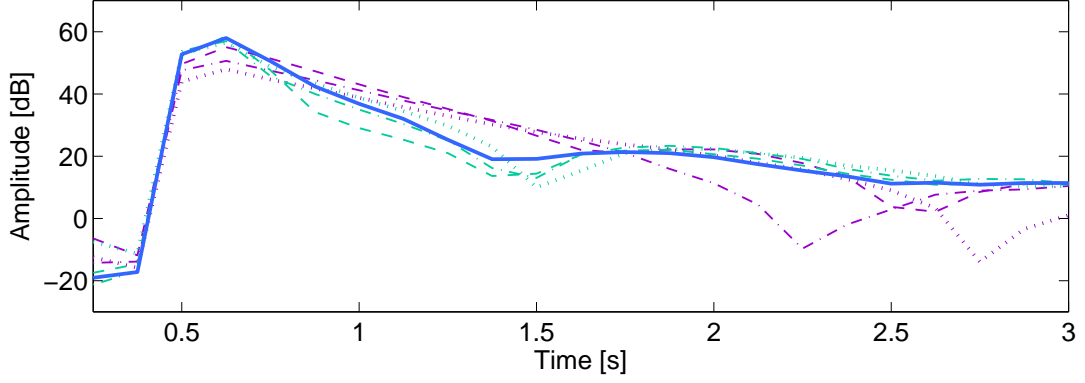
(b) Measured temporal envelopes - Active control approach.

Figure 11: Temporal envelopes of the second partial of the A string. Reference case [——], frequency altered by -15% [·····], -10% [·—·], -5% [———] and frequency altered by $+5\%$ [——], $+10\%$ [·—], $+15\%$ [·····].

lower for the control approach.

Figure 12 gives the maximum amplitude and the slope of the temporal envelope of the second partial of the string for each frequency shift. Figure 12(a) shows that the maximum amplitude of the partial increases when the frequency of the body mode is moved closer to the frequency of the partial. The maximum amplitude is reached for the $+5\%$ shift while

(a) Maximum amplitudes normalized between 0 and 1.
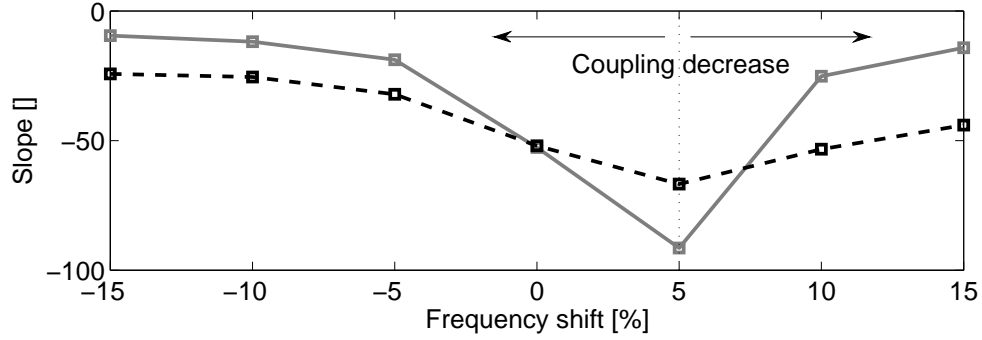
(b) Slopes calculated using 0.5 second of the temporal envelope after its maximum amplitude.

Figure 12: Maximum amplitude and slope of the temporal envelopes given in Figure 11 for the synthesis approach [——] and the control approach [- - -] and for the different shifts of the frequency.

the frequency of the controlled body mode should be approximately 223 Hz. Figure 12(b) shows that the slope of the partial also increases when the frequency of the body mode is moved closer to its frequency. Figure 11(b) shows that this slope is modified by more complex phenomena after few seconds. However, it seems that the closer are the frequencies of the body and the string modes, the quicker is the decrease of the partial. According to the conclusion of Section III.A, the coupling is strong in the reference case and decreases when

the frequency of the mode is moved away from the frequency of the partial. However it is not possible to give the split between strong and weak coupling since no specific features is observed. Once again, it should be noticed that the modification of the coupling between the string and the mode of the soundboard depends on the initial coupling conditions. The results would have been different if the coupling of the reference case has not been strong.

IV. DISCUSSION

The two proposed approaches seem to be efficient ways to study complex phenomena like the sound production of musical instruments. The previous sections reveal that each approach has its own advantages and drawbacks. The choice of the method depends on the targeted goal.

On a real instrument, a lot of parameters like the temperature or the humidity can modify the mechanical properties of the studied structure. In the model used in the synthesis approach, these parameters are fixed by the user as it is shown in section II.B. If the influence of one of these parameters has to be studied, it is possible to modify it without changing the others. This is not always possible with active control. For example, Figure 8 reveals that the modal frequency can be modified without changing the damping factor for the synthesis approach but not for the control approach. Synthesis is also really convenient to study the influence of a wide range of parameters. In section II.B, a lot of parameters can be modified, while the model of the control approach is focused on the properties of the soundboard. Another advantage of synthesis is to enable the modification of the model parameters until extreme limits that are impossible to reach with modal active control, which is limited by the quality of the computation, the energy needed to reach a control target, and by the real-time

requirements.

However, it is not possible to play or to listen the sound of the synthesis method as the sound of a real instrument. Controllers (like computers or MIDI keyboards) and sound emission systems (like loudspeakers or headphones) are one of the limits of the sound synthesis. To be used in psychoacoustical tests, the sound synthesis must be realistic, thus needing a very complex physical model (plucked string, soundboard, sound radiation, etc). Results from sound synthesis must be compared to more reliable ones, coming generally from experimental data. As the modal active control only needs the knowledge of the modes of vibration of the soundboard, it does not need a physical model of a complete instrument. For the modal active control method, the modeling step is much easier and less complicated (although limited to linear control theory). The realism is not an issue for the active control approach, since the modifications are made *in situ*, thus the sound is radiated directly by the instrument, and the instrument is still playable. Modal active control enables the study of very complex situations (multiphysics or involving human player for instance), while needing only simple models of the sub-system that is controlled (like the soundboard).

V. CONCLUSION

This paper proposes to compare two different approaches in order to modify the modal parameters of a guitar soundboard. The first one is a frequency domain synthesis method using the bridge impedance and the inverse Fast Fourier Transform. A model is used to compute the radiated sound of a plucked string fixed on a modal model of the guitar soundboard. The second one is an active control method using a linear modal state model of the controlled structure and enabling the *in situ* modifications of the modal parameters of the

guitar soundboard. This paper compares these two approaches modifying the modal damping factor and the modal frequency of the second vibration mode of the soundboard. Different modifications are studied in each case. The effects of these modifications are studied in the bridge impedance of the soundboard and in the radiated sound of the synthesized and of the controlled guitar.

The close results obtained for the two approaches are the first significant result of this study. These results are not exactly the same but they lead to the same conclusion about the influence of the modal parameters in the sound of musical instruments. Indeed, the effects of the modal modifications are similar for the two proposed approaches both in the bridge impedance and in the radiated sounds.

The second important result concerns the choice of one of these two methods according to the targeted goal of the user and knowing the characteristics of both approaches. The synthesis approach is more convenient to reach precisely the targeted modal properties, while modal active control is more realistic for studies where the whole instrument, listening and playing experience are important.

Acknowledgements

Appendix A

Tables 3 and 4 give the parameters of the string and of the air used in the model of the synthesis method.

Table 5 gives the modal parameters and the corresponding values of B and C of the first

f_{string} [Hz]	T [N]	ρ_s [kg.m^{-1}]	c_s [m.s^{-1}]	B [Nm^2]	η_F []	η_B []	η_A [s^{-1}]	L [m]
110	73.9	3.61 10^{-3}	143	40 10^{-6}	7 10^{-5}	2.5 10^{-2}	0.9	650 10^{-3}

Table 3: Parameters of the synthesized string.

c [m.s^{-1}]	ρ_{air} [kg.m^{-3}]
340	1.184

Table 4: Air parameters.

ten modes identified using the impedance measured at the bridge of the soundboard.

Mode number	f_k [Hz]	ξ_k []	$\mathbf{\Pi}_k^a$ []	$\mathbf{\Pi}_k^c$ []
1	87	0.007	0.073	1
2	113	0.029	0.166	1
3	213	0.025	1.254	1
4	232	0.009	0.105	1
5	271	0.007	0.074	1
6	378	0.008	0.078	1
7	409	0.019	0.031	1
8	418	0.014	0.218	1
9	504	0.011	0.141	1
10	563	0.013	0.091	1

Table 5: Modal parameters of the first ten modes of the soundboard.

REFERENCES

1. E. V. Jansson, "Admittance Measurements of 25 High Quality Violins", Acta Acustica united with Acustica, **83**: 337-341 (1997).

2. C. E. Gough, "The Resonant Response of a Violin G-string and the Excitation of the Wolf-Note", Acta Acustica united with Acustica, **44**: (1980).

3. C. E. Gough, "The Theory of String Resonances on Musical Instruments", Acta Acustica united with Acustica, **49**: 124-141, (1981).

4. J. Woodhouse, "On the Synthesis of Guitar Plucks", Acta Acustica united with Acustica, **90**(5): 928-944, (2004).

5. J. Woodhouse, "Plucked Guitar Transients: Comparison of Measurements and Synthesis", Acta Acustica united with Acustica, **90**(5): 945-965, (2004).

6. J. Woodhouse, E. K. Y. Manuel, L. A. Smith, A. J. C. Wheble and C. Fritz, "Perceptual Thresholds for Acoustical Guitar Models", Acta Acustica united with Acustica, **98**: 475-486, (2012).

7. C. Fritz, I. Cross, B. C. J. Moore and J. Woodhouse, "Perceptual Thresholds for Detecting Modifications Applied to the Acoustical Properties of a Violin", Journal of The Acoustical Society of America, **122**(6), (2007).

8. H. Wright, The Acoustics and Psychoacoustics of the Guitar, University of Wales, College of Cardiff, Ph.D. Thesis, (1996).

9. S. Griffin, Acoustic Replication in Smart Structurs Using Active Structural/Acoustic Control, Georgia Institute of Technology, Department of Aerospace Engineering, Ph.D. Thesis, (1995).

10. S. Griffin, S. A. Lane and R. L. Clark, The Application of Smart Structures Toward Feedback Suppression in Amplified Acoustic Guitars, Journal of The Acoustical Society of America, **113**(6): 3188-3196, (2003).

11. C. Besnainou, "Modal Stimulation: A Sound Synthesis New Approach", Proceedings of International Symposium on Musical Acoustics, ISMA95, pp. 434-438, Dourdan, France, July, (1995).

12. H. Boutin, C. Besnainou and J.D. Polack, "Modifying the resonances of a xylophone bar using active control", Acta Acustica united with Acustica, **101**: 408-420, (2015).

13. H. Boutin and C. Besnainou, "Physical Parameters of the Violin Bridge Changed by Active Control", Journal of The Acoustical Society of America, **123**: 3656, (2008).

14. E. Berdahl, J.O. SmithIII and A Freed, "Active damping of a vibrating string", 6th International Symposium on Active Noise and Vibration Control, Adelaide, Australia, September, (2006).

15. B. Elie, F. Gautier and B. David, "Macro Parameters Describing the Mechanical Behavior of Classical Guitar", Journal of The Acoustical Society of America, **132**(6): 4013-4024, (2012).

16. A. Chaigne and J. Kergomard, Acoustique des Instruments de Musique (Acoustics of Musical Intsruments), pp. 552, Belin, Paris, France, (2008).

17. M. H. Richardson and D. L. Formenti, "Parameter Estimation from Frequency Response Measurements using Rational Fraction Polynomials", 1st IMAC Conference, Orlando, Florida, US, November, (1982).

18. A. Preumont, Vibration Control of Active Structures, An Introduction, Chap. 9, Springer-Verlag Berlin Heidelberg, Germany, (2011).

19. W. K. Gawronski, Dynamics and Control of Structures: A Modal Approach, 232 pages, Springer-Verlag New-York, US, (1998).

20. S. Benacchio, B. Chomette, A. Mamou-Mani and V. Finel, "Mode Tuning of a

Simplified String Instrument Using Time-Dimensionless State-Derivative Control",
Journal of Sound and Vibration, **334**: 178-189, (2015).

21. T. Meurisse, A. Mamou-Mani, S. Benacchio, B. Chomette, V. Finel, D. B. Sharp and
R. Causs, "Experimental demonstration of the Modification of the Resonances of a
Simplified Self-Sustained Wind Instrument Through Modal Active Control", Acta
Acustica united with Acustica, **101**: 581-593, (2015).

22. J. Kautsky, N. K. Nichols and P. Van Dooren, "Robust Pole Assignement in Linear
State Feedback", International Journal of Control, **41**(5): 1120-1155, (1985).

23. T. H. S. Abdelaziz, "Robust Pole Assignment for Linear Time-invariant Systems
using State-derivative Feedback", Journal of Systems and Control Engineering,
223(2): 187-199, (2009).

24. D. G. Luenberger, "Observing the State of a Linear System", Military Electronics,
IEEE Transactions on, **8**(2): 74-80, (1964).

List of Figures

List of Tables